

# State-specific complete active space multireference Møller–Plesset perturbation approach for multireference situations: illustrating the bond breaking in hydrogen halides

Sudip Chattopadhyay · Uttam Sinha Mahapatra ·  
Rajat K. Chaudhuri

Received: 21 August 2011 / Accepted: 23 March 2012 / Published online: 15 April 2012  
© Springer-Verlag 2012

**Abstract** Assessment of the complete active space-based state-specific multireference Møller–Plesset perturbation theory, SS-MRMPPT, has been performed on the ground states of HX (X = F, Cl, and Br) systems through the computation of potential energy surface (PES) and spectroscopic constants (such as equilibrium bond lengths, rotational constants, centrifugal distortion constants, vibrational frequencies, anharmonicity constants, and dissociation energies that are closely related to the shape and accuracy of the energy surfaces) extracted from the computed PES. The SS-MRMPPT (involves multiple amplitude sets to parametrize the exact wavefunction) approach isolates one of the several states provided by an effective Hamiltonian in an attempt to avert intruder states in size-extensive manner and hence it forms the basis of a robust approach to the electron correlation problem in cases where a multireference formalism is required. The absence of intruder problem makes SS-MRMPPT an interesting choice for the calculation of the dissociation energy surface(s). The performance of the method has been judged by comparing the results with calculations provided by current generation *ab initio* methods (multireference or single-reference methods) and we found, in general, a very good

accordance between them which clearly demonstrates the usefulness of the SS-MRMPPT method.

**Keywords** Multireference perturbation theory · Møller–Plesset partitioning · Intruder effect · Potential energy surfaces · Spectroscopic parameters · Hydrogen halides

## 1 Introduction

In recent times, multireference (multiconfiguration) electronic systems [described by the wavefunctions that are not even qualitatively approximated by a single Hartree-Fock (HF) function] have attracted much attention in the fields of chemical (and material) sciences as they are abundant in chemistry.<sup>1</sup> Multireference situations often occur, for example, in the mapping of complete reaction paths, in the vicinity of conical intersections, during bond breaking, in free radical chemistry, electronic excited states, and so on. Over the past few decades, there has been a sustained and continuous effort to develop reliable and robust multireference (MR) methods for describing such systems or situations (see [1] for an excellent overview and extensive bibliography). Compared to multireference configuration interaction (MRCI) [2], multireference perturbation theory (MRPT) methods scale better with the system size. From its inception, MRPT represents a very useful yet relatively inexpensive tool to investigate MR systems [3] retaining

S. Chattopadhyay (✉)  
Department of Chemistry, Bengal Engineering and Science  
University, Shibpur, Howrah 711103, India  
e-mail: sudip\_chattopadhyay@rediffmail.com

U. S. Mahapatra  
Department of Physics, Maulana Azad College, 8 Rafi Ahmed  
Kidwai Road, Kolkata 700013, India  
e-mail: uttam.mahapatra@linuxmail.org

R. K. Chaudhuri  
Indian Institute of Astrophysics, Bangalore 560034, India  
e-mail: rkchaudh@iiap.res.in

<sup>1</sup> Of course, the use of genuine multireference methods presents additional levels of complexity for the practitioners, when compared with the corresponding single-reference methods. The genuine multireference approaches often require a degree of subjective judgment from the user to render the calculations manageable and effective. The most obvious conceptual challenge is to choose a meaningful active space for describing a given chemical problem.

*ab initio* accuracy as it deals with two types of electron correlation, nondynamic and dynamic,<sup>2</sup> in a balanced and effective way. It should be mentioned here that the effects of dynamical and nondynamical correlations are not additive and need a coupled and balanced treatment for both. In contrast to single-reference PT (SRPT) [4, 5], MRPT is not uniquely defined and consequently, MRPT methods exist in a number of variants [6–37], the developments being carried on continuously. There are various pro and contra issues for different MRPT methods, which shape their numerical demands. The state-specific MRPT (SS-MRPT) method, initially developed and implemented by Mahapatra-Datta-Mukherjee [28, 29, 38] and later pursued by our group [39–44], appears as an efficient and useful approach to study many chemical problems [38–48]. Among the multitude of MRPT approaches, the SS-MRPT method suggested by Mahapatra et al. [28, 29] holds a lot of appealing features such as (1) it is able to treat nondynamical and dynamical correlation effects in a balanced and accurate manner (2) it is insensitive toward the intruder states problem<sup>3</sup> [49–51] yet allowing relaxation of zero-order wavefunction within a model space (i.e., providing fully relaxed treatment of the nondynamical correlation where the CI coefficients of the active functions are iteratively updated as dynamical correlation) (3) it is both size-extensive and size-consistent (when one uses orbitals

<sup>2</sup> Nondynamic correlation is associated with the strongly interacting reference determinants or configurations (via linear combination of the reference functions) while the dynamic one gives contributions to the wave function from the space orthogonal to that spanned by the reference functions, i.e., arising from the couplings between the model and outer spaces. Electronic structure methods capable of providing ‘chemical accuracy’ for ground and electronically excited states of molecules must include both dynamical and nondynamical correlation effects.

<sup>3</sup> Intruder problem is ubiquitous in studying potential energy surfaces leading to the formulation of molecules. In the multireference perturbation theory, intruder state problems (causing appearance of very small energy denominators in PT series and leading to spurious results of the entire PT calculations) are inevitable from the theoretical point of view. On the other hand, for multireference coupled cluster method based on the generalized Bloch equation, intruder problem is a consequence of the polynomial character of amplitude finding equations due to the exponential ansatz for the wave function. Not only that, nonlinear character of the Bloch equation also invites the existence of multiple solutions. Electronic structure methods capable of providing chemical accuracy for ground and excited states of atoms or molecules must be free from such effects. The intruder state problem can usually be corrected by widening the model space, but this inevitably leads to an increase of the computational effort. The main essence of the development of MR-based theory is to employ as small an active or reference space as possible. A well-established workaround for this problem is to focus on one single state of the effective Hamiltonian, leading to state-specific methodology. In most cases, the influence of intruder states becomes more important away from equilibrium regions and successful treatment of this issue will influence the accuracy of predicted energies.

localized on the separate fragments), and (4) It is spin-free (applicable to both ground and excited states with either closed-shell or open-shell configurations). It is worth noting that the different variants of MRPT [say CASPT2 (second-order complete active space perturbation theory) [6–8], MRMP2 (second-order multireference Møller–Plesset perturbation theory) [9–12] and its multistate variant, referred to as MCQDPT (multiconfiguration quasidegenerate perturbation theory) [13] approaches by and large avoid the size-consistency error, but not rigorously [52–55]. Recently, Evangelista et al. [45] demonstrated that the SS-MRPT theory is particularly useful in MR focal point extrapolations to determine *ab initio* limits (quickly converges to the full CI limit). For these reasons, SS-MRPT could represent a reliable approach to model any region of the potential energy surface (PES)<sup>4</sup> of a molecular system (with closed/open-shell and singlets/non-singlets model functions) even when the traditional effective Hamiltonian-based MR methods fail due to intruders and hence has the potential to serve as theoretical basis for the routine investigation of molecular systems, in which strong static electron correlation is present. All the tests on the SS-MRPT approach that have been carried out so far [28, 29, 38–48] clearly demonstrate the effectiveness of this method in handling of the MR ground and excited states with either closed- or open-shell nature even for medium-size molecular systems at a low computational cost, yielding acceptably good results that can be meaningfully compared with the established computationally expensive full-blown coupled cluster (CC) estimates. At this point, it is worth pointing out that the accuracy and applicability of the SS-MRPT have been tested numerically on certain representative examples in light of other MRPT methods like the one by Chaudhuri et al. [56] and Hoffmann et al. [46]. In the present paper, we further examine the performance of the SS-MRPT within the framework of multipartitioning Møller–Plesset (MP) scheme [57–59] using Rayleigh–Schrödinger (RS) perturbative expansion, (coined as SS-MRMPPT) in computations of the HX (X = F, Cl, and Br) dissociation potentials, some involving a heavy atom. The RS variant of SS-MRPT proposed by Mukherjee and coworkers stems by a linearization of the amplitude equations of their full-blown SS-MRCC method [28]. We remark here that the emergence of the SS-MRPT equations considered here is not based on a rigorous order-by-order analysis of the parent SS-MRCC equations [28].

<sup>4</sup> The energy and behavior of a molecule can be expressed as a function of the positions of the nuclei, that is, a potential energy surface and hence many aspects of chemistry can be reduced to questions about potential energy surfaces. A potential energy surface arises naturally when the Born–Oppenheimer approximation is invoked in the solution of the Schrödinger equation for a molecular system.

SS-MRMPPT is seen as a remedy to a problem which plagues the traditional multireference RS perturbation theory—the so-called intruder state problem.<sup>5</sup> The availability of a large number of theoretical studies, including several CC calculations of the HX spectroscopic parameters, makes these molecules good model systems for testing the performance of a new method. To proceed further, we recall briefly the essential ingredients and structural aspects of the formulation of the SS-MRMPPT used which has been published in detail previously [28, 29, 38–44].

The following presentation serves (1) to provide the necessary background (salient methodological aspects), (2) to introduce our notation, and (3) to describe the unique advantages of the SS-MRMPPT approach to study the correlation problem for systems requiring a multireference formalism. Additional details can be found in the original papers on this theory [28, 29]. The principal idea of the state-specific MR approach (say SS-MRPT) is to solve the Schrödinger equation to obtain only the target eigenvalue out of the whole spectrum. We present here a brief summary of the main ingredients of the formulation. SS-MRPT operates with the Jeziorski–Monkhorst (JM) parametrization of the wavefunction [60, 61]<sup>6</sup>

$$\psi = \sum_{\mu} \exp(T^{\mu})|\phi_{\mu}\rangle c_{\mu} \quad (1)$$

and assumes the existence of a complete active space (CAS) wave function written as  $\psi_0 = \sum_{\mu} c_{\mu}|\phi_{\mu}\rangle$ . In the case of the spin-adapted version of SS-MRMPPT [38–44], each model space function  $\phi_{\mu}$  is a configuration state function (CSF) in a given spin-coupling scheme. The spin-adaptation of the equations in such cases is straightforward and trivial, entirely analogous to the one for the case of closed-shell SRPT. Using Eq. (1), geared specifically to treat a single electronic state, leads to the state-specific (SS) MR methods. Here,  $c_{\mu}$ 's are the combining coefficients of the model space functions. The cluster operator  $T^{\mu}$  (defined with respect to the  $\mu$ -th reference configuration as the respective Fermi vacuum), by its action on  $\phi_{\mu}$ , leads to various virtual functions  $\chi_l^{\mu}$  with attendant cluster amplitudes  $t_{\mu}^l$ . The intermediate normalization is here assumed, which translates to the requirement of zero amplitudes for internal excitations in the case of complete model space. In SSMR method, all the parameters entering into the wave function ansatz are optimized for a specific or desired electronic states. In SS-

MRMPPT theory [28, 29, 38], the Hilbert space-based perturbation theory is reduced to a state-specific formalism through an amplitude equation to determine the cluster operator as (that should hold for each  $\mu$  and  $l$ )<sup>7</sup>

$$t_{\mu}^{l(1)}(\mu) = \frac{H_{l\mu}}{[E_0 - H_{ll}]} + \frac{\sum_{v \neq \mu} t_{\mu}^{l(1)}(v) H_{\mu v} (c_v^0 / c_{\mu}^0)}{[E_0 - H_{ll}]} \quad (2)$$

where  $E_0$  and  $c_{\mu}^0$  denote unperturbed state energy (corresponds to the CAS energy) and the frozen (zero-order) model space coefficient(s), respectively. Eq. (2) indicates explicit dependence of the cluster amplitudes on the zeroth-order coefficients  $c_{\mu}^0$  for the state of interest. This shows that the working equations for the cluster amplitudes are indeed *state-specific* in nature. In the above-mentioned cluster finding equation, we have used the following notations:  $\langle \chi_l^{\mu} | T_{\mu}^{l(1)} | \phi_{\mu} \rangle = t_{\mu}^{l(1)}(\mu)$ ,  $\langle \chi_l^{\mu} | T_v^{l(1)} | \phi_{\mu} \rangle = t_{\mu}^{l(1)}(v)$ ,  $\langle \chi_l^{\mu} | H | \phi_{\mu} \rangle = H_{l\mu}^{\mu}$ , and  $\langle \chi_l^{\mu} | H_0 | \chi_l^{\mu} \rangle = H_{ll}^{\mu}$ . We emphasize here that in the SS-MRMPPT formalism, every CSF is associated with its own cluster excitation operator to take care of the differential and the dynamical correlation effects, instead of applying one universal operator to the whole reference function. Equation (2) is coupled nonlinear equation involving various cluster amplitudes (and the model space coefficients) and we note that the only coupling between the various  $T_{\mu}$ s is via the sum over  $v$  appearing in the numerator of the above equation. There is thus no coupling between the various excitation components in  $T^{\mu}$ s, and the coupling is present with only those  $T^{\nu}$ s which lead to the same excitation as by the product of excitation operators for the specific  $t_{\mu}^{l(1)}$  under consideration. Thus, no cluster amplitudes need to be stored in the formulation considered here.

The second-order perturbation equation for the energy (with the restriction that only one root of the effective Hamiltonian is physically meaningful) is given by

$$\sum_v \tilde{H}_{\mu v}^{(2)} c_v = E^{(2)} c_{\mu} \quad (3)$$

where  $\tilde{H}_{\mu v}^{(2)} (= H_{\mu v} + \sum_l H_{\mu l} t_v^{l(1)}(v))$  denotes reference-specific dressed Hamiltonian. A typical feature of the

<sup>5</sup> Traditional multireference Rayleigh–Schrödinger perturbation theory is designed to describe a manifold of states. However, as the perturbation is switched on the relative disposition of these states and those states outside the reference space may change in such a way that convergence of the perturbation series is impaired or even destroyed.

<sup>6</sup> This ansatz was first introduced by Jeziorski and Monkhorst in the context of state-universal multireference coupled cluster.

<sup>7</sup> In SSMR formulation as, via the JM ansatz, every virtual function is generated from each model function by the action of a cluster operator of suitable excitation rank, there is an inherent redundancy of the number of cluster amplitudes *vis-a-vis* the corresponding configuration interaction coefficients accompanying the virtual function (needed to fully characterize the eigenfunction  $\psi$ ). Using sufficiency conditions satisfying some important physical requirements (such as the theory be free from intruders and be rigorously size-extensive) Mukherjee et al. developed the SS-MRPT method [28, 29] by invoking a partition of  $H$  into  $H_0$  (a zeroth-order part) and  $V$  (a perturbation), and an order-by-order expansion of cluster operators,  $T^{\mu}$  of their SS-MRCC formalism [28]. Although sufficiency condition proposed by Mukherjee et al. is very useful, the underlying physical meaning still evades a clear understanding.

SS-MRMPPT formalism up to second order of energy is the use of the zeroth-order coefficients to compute the cluster operators and  $\tilde{H}$ , but allow the coefficients to relax while computing  $E^{(2)}$ , since this is obtained by diagonalization [via Eq. (3)]. SS-MRMPPT uses the relaxed coefficients  $c_\mu$  (as it is more general), rather than some pre-computed set of frozen coefficients  $c_\mu^0$ . Hence, the SS-MRPT formulation provides a completely relaxed form of  $\psi$ . It is thus able to deal with the mixed-states problem, characterized by large changes in the relative contributions of the coefficients of reference functions in the correlated final wave function compared to the zero-order function. In the present paper, all SS-MRMPPT calculations were carried out using relaxed description. We should mention here that the SS-MRMPPT method considered here is completely flexible in the sense that one can use it to compute the energy either as an expectation value with respect to the unrelaxed or frozen function (akin to CASPT2 or MRMP2):  $E^{(2)} = \sum_{\mu,\nu} c_\mu^0 \tilde{H}_{\mu\nu}^{(2)} c_\nu^0$ , where  $c_\mu^0$  stands for the unrelaxed coefficients of the reference functions. In the case of large CAS, the unrelaxed method has computational merits as compared with the relaxed one, diagonalization of large matrix is not necessary.<sup>8</sup> The unrelaxed description of CASPT2 and MRMP2 methods can be converted into the corresponding relaxed ones with generalizations for the multistate variants (MS-CASPT2 and MCQDPT), in which the wavefunctions of different states are allowed to mix [13, 36, 62, 63].

In SS-MRPT method, the denominator of the cluster finding equation, Eq. (2) guarantees the existence of a natural gap, and this characteristic allows the intruder state problem to be avoided and convergence of the perturbation series occurs in a natural way (without having to add an arbitrary shift in the denominator), irrespective of whether the state of interest is ground or excited, as long as the unperturbed energy  $E_0$  is rather well removed from the energies of states evolving from the virtual spaces. It is noteworthy that this aspect for the avoidance of intruder states can almost always be met for ground state, but is a much trickier issue for the computation of the excited states. In the case of the excited state(s), more iteration steps are required (which are application specific) to obtain convergence of the equations as compared to the ground state. Convergence of the iterative steps required is

reasonably fast for all cases reported here. Recently, Evangelista et al. [45] have shown (via the calculation of the time required to compute the second-order energy) that the iterative solution of the SS-MRPT amplitude equations is not a bottleneck. It is pertinent to mention that the persistence of the intruder problem varies with the particular MRPT approach. For instance, it has been demonstrated in [64, 65] that NEVPT2 (second-order n-electron valence state perturbation theory) [19–22] is inherently less sensitive to this problem as compared with MRMP2 [9–12] and CASPT2 [6–8]. In this context, we also mentioned the observations of the convergence of MRPT, in particular the CASPT method by Olsen and Fülischer [66]. A study of the convergence of Møller–Plesset MRPT in CI spaces restricted to single and double excitations from a CAS reference has been reported by van-Dam and van-Lente [67]. They argue for the use of the convergence of the MRPT in this restricted space, as an indicator of the convergence of the perturbation expansion in the full space.

A key issue in MRPT concerns the definition of a proper zero-order Hamiltonian,  $H_0$  (rather  $H_0^\mu$ ).<sup>9</sup> The efficacy and generality of a perturbative method depends on the choice of the unperturbed Hamiltonian. We use a type of reference-related Fock-like operator based on the concept of multipartitioning scheme [57–59]. We employ the following vacuum-dependent Fock operator [39–44]:

$$f_\mu = \sum_{ij} \left[ f_{\text{core}}^{ij} + \sum_u \left( V_{iu}^{ju} - \frac{1}{2} V_{iu}^{uj} \right) D_{uu}^\mu \right] \{E_i^j\} \quad (4)$$

The operators  $E$  in curly brackets denote the normal ordering with respect to the vacuum. In Eq. (4),  $u$  describes both a doubly occupied and a singly occupied active orbital in  $\phi_\mu$ , and  $D^\mu$ s are the densities in the CSF space labeled by the active orbitals where  $i, j, \dots$  refer to spatial orbitals. The  $D^\mu$ s are computed first and stored in the fast memory which are used in the construction of the reference space Hamiltonian matrix elements and second-order pseudo effective operators  $\tilde{H}$ . All other density matrix elements (say two and three body) are computed on the fly during computation. As our  $H_0$  is always diagonal (as for MP scheme), the zero-order Hamiltonian operator is:  $H_0^\mu = \sum_i f_\mu^{ii} \{E_i^i\}$ . For such a  $H_0$ , the cluster amplitudes of particular classes are decoupled from other classes in the first-

<sup>8</sup> In a unrelaxed (frozen) treatment, the updating of the nondynamical correlation as a result of mixing of the virtual functions is not done, assuming approximate additivity of the two effects and thus the methods of frozen coefficients variety (unrelaxed version) may suffer from the internal contraction of the wave function in the reference space. The relaxed (internally decontracted) treatment, on the other hand, dresses the effective operator in the active space, and the diagonalization of this operator automatically relaxes the coefficients of the model functions.

<sup>9</sup> A general difficulty of MRPT is the choice of the zeroth-order Hamiltonian. This is less straightforward than in the SR-based Møller–Plesset perturbation theory, since in the multireference case there is no one-electron Fock operator which is diagonal in the orbital basis. Thus, the zeroth-order Hamiltonian is in general nondiagonal, and a set of linear equations must be solved to determine the first-order wave function. Alternatively, the off-diagonal elements of the zeroth-order Hamiltonian can be neglected, but this may cause additional errors and removes orbital invariance properties.



order perturbation (for a detail discussion along these lines, see [38]). It is also worth commenting that our partitioning preserves the structure of the single-reference  $MP_n$  series (i.e., the direct terms have the same form) and because of the presence of coupling terms, it leads to equations (Eq. 2) that require an iterative solution. In a number of applications, it has been shown that the Fock operator in Eq. (4) gives an acceptably good descriptions of the ground and electronically excited states [39–44].

We have further scrutinized the quality of the computed PESs through the computation of molecular spectroscopic parameters. Such an attempt also probes the performance of our SS-MRMPPT calculations in a more realistic way. The calculations of PESs and the spectroscopic parameters are sensitive to several factors, viz. (a) the effectiveness of the method used to describe the dynamic and nondynamic electron correlation effects in a balanced fashion, (b) the quality of the basis set used in the calculations, and (c) the accuracy of the fit or analysis employed to approximate the PES in the subsequent calculation of the spectroscopic constants. In addition, the number of points used in the PES fitting may influence the accuracy of the calculation of the spectroscopic parameters. From the data displayed in [68]<sup>10</sup> for HX systems [via the third-order Douglas–Kroll (DK) relativistic CC theory with a series of correlation-consistent basis sets including the largest set of atomic basis functions that is technically feasible], it is clear that the use of larger-size basis sets and the use of methods capable to handle correction effects efficiently over the entire energy surface are crucial in achieving spectroscopic parameters with experimental accuracy. The energy surface and equilibrium internuclear separation ( $R_e$ ), harmonic frequency ( $\omega_e$ ), rotational constants ( $B_e$ ), centrifugal distortion constants ( $D_e$ ), and dissociation energy ( $D_0$ ) of the ground-state HX molecules have been investigated using the SS-MRMPPT approach in combination with different basis sets of Dunning et al. [69–71] (cc-pVQZ, cc-pV5Z (-h), aug-cc-pVTZ, aug-cc-pVQZ, aug-cc-p5Z(-h) [h shell was removed because used versions of GAMESS(US) do not support h shells] for HF molecule, and aug-cc-pVDZ and aug-cc-pVTZ for HCl and HBr molecules). Going beyond the necessarily modest basis sets that are used in FCI comparisons is obviously essential if meaningful comparisons are to be made with experiment. The basis sets used (standard contracted variants) in this paper were taken from. [72, 73].<sup>11</sup> The equilibrium harmonic frequencies  $\omega_e$ , given essentially by the curvature of the PES at  $R_e$ , represent perhaps the most sensitive test of the quality of the computed potentials. The calculated dissociation

energy (which strongly depends on the quality of the energy calculated at a large internuclear separation) has been computed by subtracting the energy at a large interatomic distance from that at  $R_e$ . It is important to note that the determination of bond dissociation energies is of crucial importance for any discussion of thermodynamic equilibrium constants. Comparing the calculated values of spectroscopic constants with the experimental values (taken from Huber and Herzberg [74]) enables one to do the following: (a) test the quality of the computed PES; and (b) if some system exhibits a significant difference between the calculated value and the experimental value, it can provide a clue that there may be some peculiarity in the computed PES. The other issue of this work is to assess the performance of the SS-MRMPPT method, in particular, whether in the presence of multireference character it performs as well as the standard MR-based approach does, and gives better results in situations in which the ‘gold standard’ CCSD(T) is inadequate. Whenever possible, we also compare the performance of SS-MRMPPT with that of estimates obtained by previously published *state-of-the-art* methods.<sup>12</sup> In the applications of the SS-MRMPPT method, molecular orbitals, two-electron integrals, the core-Hamiltonian matrices have all been computed via GAMESS(US) program package (a non-commercial quantum chemistry package) [75, 76]. We also computed the density matrix elements from GAMESS(US) package. Both MO integrals and one-body density matrix elements have been stored to the fast memory (two- and three-body matrix elements are computed on the fly during calculations) and are then read by the SS-MRMPPT calculations. We should be mentioned that the disk space required for solving SS-MRMPPT amplitude equation is negligible in comparison with that needed for storing two-electron integrals. Thus, the time required to compute the SS-MRMPPT energy is very small compared to the time needed for the entire computation of the integral transformation, the CASSCF procedure, and the generation of the two-electron integrals.

<sup>12</sup> To assess the comparative performances of electronic structure methods from a perfectly quantitative standpoint, one needs to use the same basis, the same kind of orbitals, and the same geometry. Thereby, one can avoid, or at least attenuate, differences stemming out of the theoretical artifacts while comparing the results. A rigorous comparison of our results with other methods considered here, however, is difficult due to the use of different basis sets. For this reason, the quality of our comparison may not be appropriate. It should be noted that, in this article, our aim is not to look at our method only from the quantitative standpoint. Instead, we attempt to put forth the more qualitative aspect of the method in terms of its predictive power *vis-a-vis* other standard and established methods in routine use. In view of this, we have also collected the values provided by various methods with different basis and orbitals. To judge our results qualitatively, we also consider the results of various methods with different schemes just as a reference.

<sup>10</sup> To the best of our knowledge, these spectroscopic results are the most complete and accurate ones to this day.

<sup>11</sup> See <http://www.emsl.pnl.gov/forms/basisform.html>.

We are now in position to discuss the layout of the numerical strategy that we adopt to apply the SS-MRMPPT approach. As we have already mentioned, the entire set of cluster amplitudes contained within operator  $T_\mu$  are segmented in different classes (eleven in number see [38]) and coupling between  $t'_\mu$  and  $t'_\nu$  exists when the amplitudes belong to the same class and within the domain of same excitation structure. For example,  $t_{\mu\alpha\beta}^{pq}$  and  $t_{\nu\alpha\beta}^{pq}$  are coupled, where following the customary terminology,  $(\alpha, \beta)$  represents the inactive orbitals, and  $(p, q)$  are occupied and unoccupied, respectively, in  $\phi_\mu$  and  $\phi_\nu$ . If  $u$  is identified as an active orbital which is occupied both in  $\phi_\mu$  and  $\phi_\nu$  and  $v$  is active unoccupied orbital in those functions, so that both  $t_{\mu\alpha u}^{pv}$  and  $t_{\nu\alpha u}^{pv}$  are coupled through as they belong to the same class and same excitation structure. We compute the cluster amplitudes of each class with a given excitation structure and incorporate its effect on the effective Hamiltonian matrix, so that the cluster amplitudes are computed on the fly and are not stored. So the overall computational effort depends on the effort given for all such class. We will discuss two of them here. We consider the two-body cluster operators involving inactive hole and inactive particle orbitals: some iterations are needed for the convergence of  $t_{\mu\alpha\beta}^{pq}$  (to include the effect of the coupling term) and this class contributes to the diagonal terms of the effective Hamiltonian. So the computational effort for this class scales as  $nit * N * n_d^2 * n_v^2$  where  $n_d$  and  $n_v$  described the number of doubly occupied and virtual orbitals, respectively. Here,  $nit$  is the number of iteration needed for the convergence of cluster amplitude (typically of the order of 10, though it depends on the class and structure of amplitudes concerned). We take another class of cluster amplitudes which involves active orbitals, say,  $t_{\mu\alpha u}^{pv}$ . These contribute to both diagonal and up to two-body off-diagonal matrix elements of the effective Hamiltonian. The computational effort scales as  $nit * N * N * n_d * n_v * n_a^4$  ( $n_a$  stands for the number of active orbitals), provided the non-zero two-body density matrix elements ( $D_{\mu\nu\kappa\lambda}^{IJ} = \langle \phi_\mu | E_{\kappa\lambda}^{IJ} | \phi_\nu \rangle$ , where  $E_{\kappa\lambda}^{IJ}$ 's are spin-free excitation operator) are computed a priori and stored in the fast memory.

The rest of the paper is organized as follows. The SS-MRMPPT results for individual systems considered here, as well as, the discussion of important general aspects that emerged from our present measurements in the light of previously reported values (wherever applicable or available) has been presented in Sect. 2. An emphasis is given on the quality of the computed potentials in a broad range of internuclear separations and on the computed spectroscopic constants. Spectroscopic constants ( $B_e$ ,  $\omega_e$  and  $\omega_e x_e$ ) have been computed using a standard Dunham analysis [77, 78]. Then, the rotational constant ( $B_e$ ) and centrifugal distortion constant ( $D_e$ ) have been calculated by

the relations:  $B_e = \frac{1}{2\mu R_e^2}$  and  $D_e = \frac{4B_e^3}{\omega_e^2}$  respectively (for details see [68]). In this section, we submit that the SS-MRMPPT method is a robust and useful approach to the electron correlation problem for cases where not only a multireference but also single-reference formalisms are appropriate. General discussions (regarding the overall performance of the method, the special treatments of small coefficients to avoid numerical instability in the working equations of SS-MRPT theory, etc) form the contents of Sects. 3 and 4 finally presents some concluding remarks.

## 2 Numerical applications and discussion

In our SS-MRMPPT calculations for HX systems, we employ a CAS(2,2) [2 electrons, 2 orbitals] consisting of a  $\sigma$  bonding and a  $\sigma^*$  antibonding orbital throughout the entire PES. This is the smallest model space that provides a qualitatively correct description of the ground states of HX. It is important to note that the essence of the MR-based theory is to employ as small an active space as possible. It is worth noting that for single-bond breaking, the variation of MR character occurs as the bond is stretched and hence offers a very effective avenue to examine the performance of various methods in handling the electron correlation in genuinely MR situations. For the ground-state HF, we have also estimated the results at the complete-basis-set (CBS) limit.<sup>13</sup>

### 2.1 Ground-state hydrogen fluoride [ $X^1\Sigma^+$ HF]

We first consider the HF molecule. The bond breaking of HF molecule has been previously studied with several single and multireference methods [78–94]. In addition, a precise experimental value is available for its different spectroscopic constants [74]. Hence, this molecule is a good model system for testing the performance of a new method. Although the ground state of HF near the equilibrium is dominated by a single configuration, however, when the H–F bond is stretched, the ‘gold standard’ CCSD(T) (CC method with singles, doubles, and perturbatively corrected triples) starts to show significant errors and is not able to produce a smooth PES of correct shape [80–82, 87]. However, Hirata et al. [90, 91] have observed that the performance of the CCSDT-R12 (R12-scheme-

<sup>13</sup> Any *ab initio* calculation inevitably involves both the basis set error (i.e., the error associated with the model employed) and the error of the method itself (i.e., the intrinsic error due to the approximations involved in the method). Thus, when comparing with the experiment, the accuracy of a given post-Hartree–Fock method can only be properly assessed when we can estimate the complete-basis-set limit. This can be accomplished—at least partially—by observing the trend of the computed results while systematically enlarging the basis set.

based CC approach with singles, doubles, and triples) and CCSDTQ-R12 (R12-scheme-based CC approach with singles, doubles, triples, and quadruples) methods is acceptably good. They have also demonstrated that the performance of the method(s) goes down when the magnitudes of the connected triples and quadruples contributions become significantly large. It is important to mention the fact that when computing energy surfaces, it is their shape that is of paramount importance, in addition to their location on the absolute energy scale. These facts indicate the clear benefit of using a genuine MR-based approach.

We have used aug-cc-pVTZ, cc-pVQZ, cc-pV5Z(-h), aug-cc-pVQZ, and aug-cc-pV5Z(-h) basis sets [72, 73] along with CAS(2,2) throughout the potential surface. The 1s core orbitals of F have been kept frozen in all calculations. Li and Paldus [80–82] have demonstrated that the effect due to the core electrons is rather insignificant. In our previous study [39–44], we have employed the smaller DZ, 6–31G\*\* and cc-pVTZ basis sets in order to enable a comparison with the full CI (FCI) results. We focus in the present study only on the results for larger and physically more meaningful basis sets with polarization orbitals.

To illustrate and quantify how well is the SS-MRMPPT approach along with different well used perturbation methods (published previously [88]) parallel to the FCI/6-31G\*\* PESs, the results are presented graphically in Fig. 1. In the inset to this figure, we also plot the results of intruder-free Brillouin-Wigner CC single–doubles (BWCCSD) studies to envisage whether the SS-MRMPPT method yields results in close agreement with MR-based CC methods or not. We realize that the SS-MRMPPT/6-31G\*\* potential nicely reproduces the available FCI potentials. Even with the minimal two-electron/two-orbital active space, SS-MRMPPT computations produce energies that are very close to those obtained with the computationally very expensive BWCCSD ones over the entire energy surface, which illustrates another useful measure for the success of SS-MRMPPT methodology. As shown in Fig. 1, the results deteriorate appreciably for the MP2/6-31G\*\* at large distances. Dutta-Sherrill [86] found the poor performance of CCSD(T) with 6-31G\*\* basis. Li and Paldus [80–82] have also noted that the CCSD(T) method does not even produce a PES having a correct shape. The poor performance of MP2 and CCSD(T) emerges from the inherent inability of the nondegenerate perturbation theory to deal with cases of strong MR nature as is pronounced at large bond distances. The results of HF system due to Li and Paldus [80–82] clearly shown that all computationally feasible SR-based correlated methods are unable to properly describe even the simplest bond breaking situation: the breaking of a single H–F bond. The graphical results given in Fig. 1 clearly indicate the superior performance of SS-MRMPPT relative to both SR- and MR-based MP2

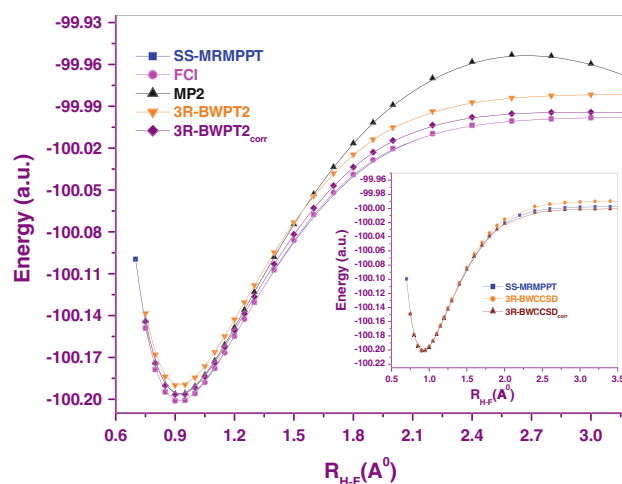


**Fig. 1** Dissociation energy surfaces of the HF molecule with the 6–31G\*\* basis set using SS-MRMPPT/CAS(2,2) along with the corresponding FCI results. We compare our results to those obtained via other allied methods

methods. As is evident from the Fig. 1, our SS-MRMPPT/6-31G\*\* calculations produce a much better energy surface in terms of its parallelism and closeness to the FCI potential (match full CI very closely around equilibrium and near dissociation which leads to very favorable shape of the PES) than do the 3 reference functions based BWPT2 (multireference, state-specific, second-order, Brillouin-Wigner perturbation theory) and BWPT2<sub>corr</sub> (*posteriori* correction for the terms which scale nonlinearly with particle number)<sup>14</sup> estimates with the same basis over the entire spectrum of nuclear separations considered here. Figure 1, also shows that the SS-MRMPPT essentially reduces to the MP2 findings around equilibrium regions, and properly corrects the inadequate behavior of MP2 in MR situations encountered in the dissociative region. The above-mentioned facts speak amply in favor of the SS-MRMPPT.

In Fig. 2, we examine the total energies of  $X^1\Sigma^+$  HF along the bond breaking coordinate obtained by the SS-MRMPPT scheme with cc-pVQZ and cc-pV5Z(-h) basis sets. We have also employed the SS-MRMPPT method to compute PESs for the HF system using basis sets of aug-cc-pVQZ and aug-cc-pV5Z(-h) quality, as one may expect the diffuse functions to be of high importance for correct description of the HF molecule in wide range of inter-nuclear distances. In this

<sup>14</sup> Although formally simple in conjunction with an explicit intruder-free nature, the BWPT2 method due to Hubáč et al. [23–25] is not rigorously size-extensive. In the first applications of BWPT2, no correction to the size-inextensivity was attempted. In a later modification, an attempt was made to expand the target energy in terms of the CASCI energy (by way of expanding the target energy in terms of an unperturbed Rayleigh–Schrödinger-like energy) to get rid of the inextensivity. This has the danger of bringing back the intruders and hence care then has to be exercised to bypass intruders.

way, we examine in Fig. 2 the basis set dependence of potential surfaces obtained at the SS-MRMPPT/CAS(2,2) level. Figure 2 shows that the topology of potential surface near the dissociation region depends considerably on the size of basis set. Therefore, such a study lends an additional way of assessing the effects of diffuse basis functions on the spectroscopic constants of HF. It is important to note that the SS-MRMPPT method provides a balanced description of the energy surface with a correct shape over the whole region of internuclear distances. Our computed PES gives a qualitative similar impression of the energy surfaces of HF at MR exp T and SRMRCC levels [89]. The energy surfaces drawn in Fig. 2 also clearly illustrate that the topological behavior of dissociation of  $X^1\Sigma^+$  HF is virtually identical with the calculations by CR-CCSD(T)/DZ [87], CCSDT-R12/aug-cc-pVDZ [90, 91] and CASCC/aug-cc-pVTZ [94] approaches. As can be observed in Fig. 2, the energy of the ground state becomes even smoother for the larger basis sets, say, cc-pV5Z(-h) and aug-cc-pV5Z(-h) showing the importance of larger basis sets. To explore the issue of smoothness of energy surface with the size and nature of the basis sets along with the nature of the orbitals, and definition of zero-order Hamiltonian in more detail, a thorough sensitivity analysis is called for. It is worth mentioning in this regard that CR-CCSD(T) [completely renormalized CCSD(T)] and CCSDT-R12 provide considerable improvements in the description of ground-state energy surface of HF when compared with the ‘gold standard’ CCSD(T) method. Li and Paldus [80–82] found that CCSD(T) utterly fails for large H–F separations.

To assess the overall quality of the computed energy surface, it is very instructive to compute spectroscopic

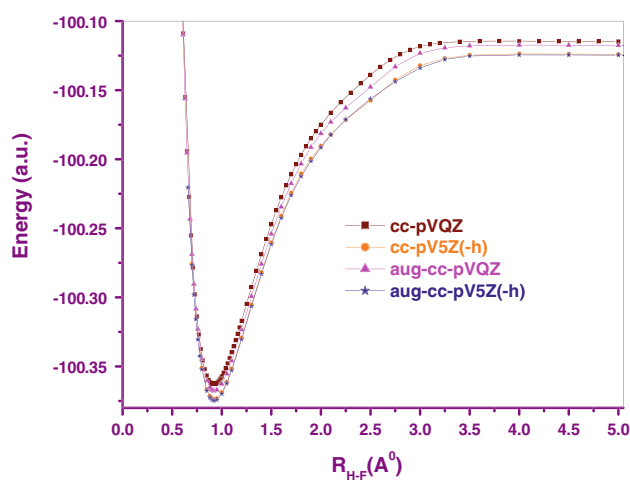


**Fig. 2** SS-MRMPPT potential energy surface of  $X^1\Sigma^+$  HF obtained with the cc-pVQZ, cc-pV5Z(-h), aug-cc-pVQZ, and aug-cc-pV5Z(-h) basis sets. Figure illustrates the basis set dependence of potential surfaces obtained at the SS-MRMPPT/CAS(2,2) level

constants and these have been assembled in Table 1 with the various correlation-consistent basis sets including cc-pV5Z(-h) one and frozen core electrons. To calibrate our spectroscopic results, we compare our present SS-MRMPPT values with the available results obtained at various sophisticated levels of electron correlation calculations. As a criterion for the effectiveness we also use the comparison of the calculated spectroscopic parameters with the experimental values.

From the previously published data due to Klopper et al. [92]<sup>15</sup> (computed at CCSD(T) level including a first-order relativistic correction obtained from an analytical evaluation of the first-order direct perturbation energy at the CCSD level in conjunction with large one-particle basis sets), it is found that the overall accuracy of the spectroscopic constants for the HF system is clearly dominated by electron correlation and basis set truncation effects, while the relativistic effects are of minor importance. Although we observe that the shapes of PESs generated via CASSCF(2,2) and SS-MRMPPT/CAS(2,2) methods are very similar, as shown in the table, the dynamical correlation effects on the spectroscopic properties of HF are noticeable. The computed spectroscopic constants are in good agreement (in conjunction with a favorable trade-off between accuracy and computational cost) with the previously published *state-of-the-art* calculations. We now focus on a comparative account of our results. The analysis emerged from the results given in Table 1 may be summarized as follows:

1. In general, the SS-MRMPPT in conjunction with larger basis sets [say cc-pVQZ, cc-pV5Z(-h), aug-cc-pVQZ, and aug-cc-pV5Z(-h)] results differ very little.
2. The SS-MRMPPT results with different basis sets show how increasing the size of basis sets affects the accuracy of the evaluation of the spectroscopic constants. Overall, our estimated spectroscopic constants for HF system move toward the experimental measurements with the increasing size of the basis set. In general, the performance of our SS-MRMPPT method is converging in nature with the size of basis sets.
3. The  $R_e$ ,  $\omega_e$ ,  $\omega_e x_e$ ,  $B_e$ ,  $D_e$  and  $D_0$  values we obtain for the  $X^1\Sigma^+$  HF are of 0.9175 Å, 4133.79, 88, 20.77, 0.00210  $\text{cm}^{-1}$ , and 158.88 (kcal/mol) at the CBS<sup>16</sup>

<sup>15</sup> In this article, authors study the difference between the various direct perturbation theory and Pauli perturbation method for the HX (X = F, Cl, Br, and I) molecules in order to investigate the relative importance of relativistic effects, higher-order electron correlation effects, and remaining basis sets effects.

<sup>16</sup> To obtain the results at CBS limit, we have used the same scheme as done by Hirata et al. [68].



**Table 1** Spectroscopic constants [equilibrium bond length  $R_e(\text{\AA})$ , vibrational frequency  $\omega_e(\text{cm}^{-1})$ , anharmonicity constant  $\omega_e x_e (\text{cm}^{-1})$ , rotational constant  $B_e(\text{cm}^{-1})$ , centrifugal distortion constants  $D_e (\text{cm}^{-1})$ , and dissociation constant  $D_0(\text{kcal/mol})$ ] for  $X^1\Sigma^+$  HF system

Ref.	Basis	Methods	$R_e$	$\omega_e$	$\omega_e x_e$	$B_e$	$D_e$	$D_0$
This work	aug-cc-pVTZ	CASSCF(2,2)	0.9158	4,233.48	105	20.36	0.00188	112.90
	cc-pVQZ	CASSCF(2,2)	0.9148	4,253.50	99	20.09	0.00179	113.45
	cc-pVTZ	SS-MRMPPT(2,2)	0.9220	3,915.07	101	20.57	0.00227	138.59
	cc-pVQZ	SS-MRMPPT(2,2)	0.9182	4,149.16	98	20.74	0.00207	152.20
	cc-pV5Z(-h)	SS-MRMPPT(2,2)	0.9178	4,140.10	92	20.76	0.00209	156.40
	aug-cc-pVTZ	SS-MRMPPT(2,2)	0.9216	4,153.44	94	20.59	0.00202	156.09
	aug-cc-pVQZ	SS-MRMPPT(2,2)	0.9200	4,112.90	99	20.65	0.00208	156.81
	aug-cc-pV5Z(-h)	SS-MRMPPT(2,2)	0.9200	4,119.02	99	20.18	0.00200	156.50
$\Delta_1$	CBS		0.001	1.8	2.12	0.2	0.00006	14.77
		SS-MRMPPT(2,2)	0.9175	4,133.79	88	20.77	0.00210	158.88
$\Delta_2$			0.0007	4.51	2.0	0.19	0.00005	17.25
Ref. [85]	cc-pVTZ	$H_{3rd}^v$	0.9155	4,184.9				118.4
Ref. [93]	6-311G**	MRMP2	0.919	4,143				131.35
		APSG-PT	0.918	4,038				134.72
		MP-pMCPT(APSG)	0.910	4,280				169.91
		MP-uMCPT(APSG)	0.916	4,160				133.49
Ref. [99]	aug-cc-pVDZ	MRCI+Q	0.9260	4,038.1				133.84
	CBS	MRCI+Q	0.9165	4,143.2				140.50
Ref. [78]	AV5Zuc	CCSD(T)	0.9173	4,142.21	89.828			–
		best calculate	0.9171	4,138.99				–
Refs. [83, 94]	aug-pVDZ	CCSD(T)	0.924(0.924)	4,084 (4,082)				134.6 (134.0)
	aug-pVTZ	CCSD(T)	0.921(0.921)	4,124 (4,123)				139.3 (138.7)
Refs. [80-82]	cc-pVQZ	4R RMR-CCSD(T)	0.9163	4,160.4	89.16	20.97		–
	cc-pVQZ	CR-CCSD(T)	0.9158	4,169.7	289.04	0.99		–
	cc-pVQZ	CCSD(T)	0.9162	4,162.1	89.00	20.97		–
Ref. [94]	aug-cc-pVTZ	CAS(2,2)CCSD	0.9194	4,138.70	89.96		0.00211	139.97
		CAS(2,2)CISD+Q	0.9194	4,127.42	92.11		0.00212	139.74
Ref. [68]	cc-pVTZ	DK3-CCSDT	0.9190	4,159	93	20.85	0.00210	128.68
		DK3-CC	0.9167	4,148	93	20.96	0.00215	134.9
Ref. [92]	aug-cc-pCV5Z	CCSD(T)+DPT(CCSD)	0.9167	4,144	90.0	20.96		
Ref. [74]		Experiment	0.9168	4,138.30	89.88	20.96	0.00215	141.63

See text for details

$H_{3rd}^v$ : Results obtained from a seven orbital reference space containing three occupied and four unoccupied valence orbitals.

Refs. [83, 84]: Values within the parenthesis correspond to the calculations made by the Dirac-Coulomb-(Gaunt) Hamiltonian

DK3-CC: Theoretical best estimate obtained from a combination of DK3-CCSD, DK3-CCSDT, DK3-CCSDTQ with the cc-pVDZ, cc-pVTZ, and cc-pVQZ basis sets [68]

$\Delta_1$ : Values correspond to the deviation of SS-MRMPPT/cc-pV5Z(-h) with respect to the experimental results

$\Delta_2$ : Values correspond to the deviation of SS-MRMPPT/CBS with respect to the experimental results

limit, respectively. The corresponding complete-correlation CBS (based on the cc-pVDZ-DK, cc-pVTZ-DK, and cc-pVQZ-DK basis sets) results with scalar relativistic and spin-orbit corrections [68] are 0.9167  $\text{\AA}$ , 4148, 93, 20.961  $\text{cm}^{-1}$ , and 134.9 kcal/mol. Thus, the spectroscopic constants obtained with the SS-MRMPPT/CBS are also in good accordance

with the values obtained by the computationally expensive calculations due to Hirata et al. [68].

4. The spectroscopic constants obtained by SS-MRMPPT with cc-pV5Z(-h) and aug-cc-pVXZ [ $XZ = QZ$  and  $5Z(-h)$ ] basis sets (and SS-MRMPPT/CBS) and CCSD(T)+DPT(CCSD)/aug-cc-pCV5Z [92] calculations are consistent with each other.

5. The errors of our computed spectral constants at CBS limit with respect to the experimental results are:  $R_e = 0.0007 \text{ \AA}$ ,  $\omega_e = 4.51 \text{ cm}^{-1}$ ,  $\omega_e x_e = 2.0 \text{ cm}^{-1}$ ,  $B_e = 0.19 \text{ cm}^{-1}$ , and  $D_e = 0.00005 \text{ cm}^{-1}$  which indicates the quality of our results. The best agreement with experiment [74] is achieved with the cc-pV5Z(-h) basis set. It should be mentioned in this context that the SS-MRMPPT(2,2) method significantly overestimates  $D_0$  (17.25 kcal/mol), in comparison with the experimental results and those from established theoretical methods. At present, the reason for this error is not clear to us. However, to eliminate, or at least, to attenuate the remaining error of SS-MRMPPT we have to implement localized orbitals (as the method is not orbital invariant and hence leads to size-consistency error with delocalized orbitals). Changing the definition of the Fockian of Eq. (4) and the expression of the renormalization term in Eq. (2) may also be expected to affect the patterns of the surface. A recent observation due to Das et al. [95], along with the desire to enhance the accuracy of the results, we consider it worthwhile to undertake an extensive survey of the SS-MRPT method with localized set of active orbitals and we expect to come back to this problem in our future publications.
6. The deviations of our SS-MRMPPT results from experimental ones never exceed  $0.005 \text{ \AA}$  for  $R_e$ ,  $223 \text{ cm}^{-1}$  for  $\omega_e$ ,  $11 \text{ cm}^{-1}$  for  $\omega_e x_e$ ,  $0.39 \text{ cm}^{-1}$  for  $B_e$ ,  $0.00012 \text{ cm}^{-1}$  for  $D_e$  and  $14.46 \text{ kcal/mol}$  for  $D_0$ .
7. In general, the SS-MRMPPT/CBS, MRCI+Q/CBS, CCSD(T)/AV5Zuc, CR-CCSD(T)/cc-pVQZ, and 4R-RMR-CCSD(T)/cc-pVQZ results differ very little.
8. The SS-MRMPPT geometries and vibrational frequencies are in close agreement with  $H_{3rd}^v$  (third-order effective valence shell Hamiltonian approach: a complete active space MRPT approach) [85].
9. Equilibrium bond distance and frequency as calculated by the MP-uMCPT due to Surján et al. [93] agree well with our predictions. However,  $D_0$  value is not well reproduced by the MP-uMCPT scheme. The harmonic frequency and dissociation energy are not well reproduced by MP-pMCPT [93].
10. In the case of a aug-cc-pVTZ basis set, the CAS(2,2)CISD[+Q] and CAS(2,2)CCSD calculations [94] yield more accurate spectroscopic constants than does SS-MRMPPT/CAS(2,2).

Considering an overall performance, we can thus say that for the ground-state HF molecule, SS-MRMPPT method performs well even at the CBS limit.

## 2.2 Ground-state hydrogen chloride [ $X^1\Sigma^+ \text{HCl}$ ]

We next consider the performance of SS-MRMPPT for the HCl molecule, using the current generation results as a benchmark. Various established wave function-based methods have been applied to investigate the HCl molecule [68, 96–100]. Here, we have used aug-cc-pVDZ and aug-cc-pVTZ basis sets [72, 73]. Although in this case the use of a much larger basis is more in order to obtain experimental accuracy, the present basis sets are reasonably adequate to enable us to draw useful conclusions regarding the applicability of the SS-MRMPPT method in PES computations. In our calculations, the Be-like core of Cl has been kept frozen. The SS-MRMPPT PESs in conjunction with aug-cc-pVDZ and aug-cc-pVTZ bases for the  $X^1\Sigma^+$  HCl have been depicted in Fig. 3. This figure clearly depicts the effect of the expansion of the basis set on the computed energy surfaces. It can be seen that the SS-MRMPPT method with different basis sets works well for the dissociation of the  $X^1\Sigma^+$  HCl molecule. Above all, topology of the SS-MRMPPT surface is almost identical to those of the corresponding highly accurate CCSDT and CR-CCSD(T) calculations with aug-cc-pVTZ basis set (where the core orbitals correlating with the  $1s$ ,  $2s$ , and  $2p$  shells of Cl have been kept frozen, and the RHF orbitals have been employed) due to Piecuch et al. [100] (see Fig. 3). As we can see, the SS-MRMPPT methods yield a good PES that is ‘almost parallel’ to the surface obtained from the CCSDT and CR-CCSD(T) methods. At this point, we should recall that the CCSDT and CR-CCSD(T)

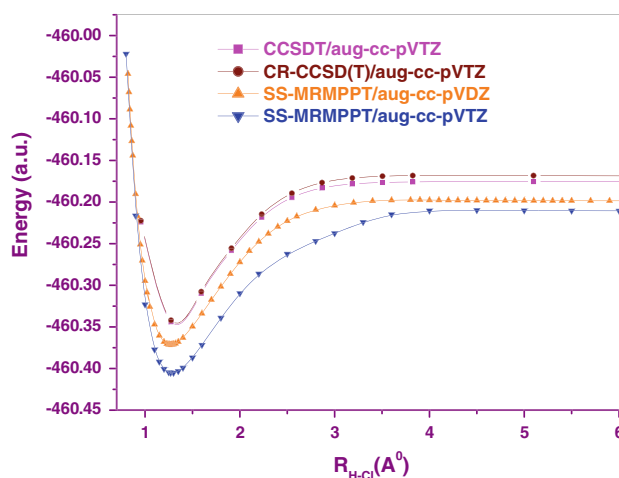


**Fig. 3** Potential energy surfaces of the  $X^1\Sigma^+$  HCl obtained with the aug-cc-pVDZ and aug-cc-pVTZ basis sets. We have also displayed the computationally demanding CCSDT and CR-CCSD(T) results with aug-cc-pVTZ basis set due to Piecuch et al. [100]. The SS-MRMPPT surface has been adjusted by 0.1 (a.u.)

**Table 2** Spectroscopic constants [equilibrium bond length  $R_e$ (Å), vibrational frequency  $\omega_e$ ( $\text{cm}^{-1}$ ), anharmonicity constant  $\omega_e x_e$  ( $\text{cm}^{-1}$ ), rotational constant  $B_e$ ( $\text{cm}^{-1}$ ), centrifugal distortion constants  $D_e$  ( $\text{cm}^{-1}$ ), and dissociation constant  $D_0$ (kcal/mol)] for  $X^1\Sigma^+$  HCl system

Ref.	Basis	Methods	$R_e$	$\omega_e$	$\omega_e x_e$	$B_e$	$D_e$	$D_0$
This work	aug-cc-pVDZ	SS-MRMPPT(2,2)	1.283	2,936	50	10.37	0.00052	110.6
	aug-cc-pVTZ	SS-MRMPPT(2,2)	1.276	2,964	49	10.49	0.00053	107.3
$\Delta$			0.001	27	4	0.10	0	0.9
Ref. [97]		ECP-SACASSCF-CI	1.2874	2,983				
		MRD-CI	1.2806	2,961				
		CEPA	1.2806	2,977				
Ref. [98]	6-311G++(3df,3p)	CAS-BCCC4	1.273	2,995				104.0
Ref. [99]	aug-cc-pVDZ	MRCI+Q	1.2938	2,966.9				100.29
	aug-cc-pVTZ	MRCI+Q	1.2790	2,975.5				104.18
	CBS	MRCI+Q	1.2769	2,978.2				106.67
Ref. [103]	cc-pVTZ	CAS-CI	1.2777	2,984.2	51.4	10.54		104.7
	cc-pV5Z	CAS-CI	1.2758	2,992.6	52.0	10.57		105.5
Ref. [68]	cc-pVQZ	DK3-CCSD	1.276	3,010	55	10.566	0.00052	99.39
	cc-pVTZ	DK3-CCSDT	1.281	2,976	56	10.486	0.00052	98.00
	cc-pVDZ	DK3-CCSDTQ	1.297	2,967	56	10.231	0.00049	91.09
		DK3-CC	1.278	2,991	55	10.541	0.00052	101.7
Ref. [92]	aug-cc-pCV5Z	CCSD(T)+DPT(CCSD)	1.2737	2,988.2	46.4	10.61		
Refs. [83, 84]	aug-pVDZ	CISD+Q	1.292 (1.292)	2,972 (2,967)				97.9 (96.9)
	aug-pVTZ	CISD+Q	1.278 (1.278)	2,999 (2,995)				103.8 (102.8)
	aug-pVDZ	CCSD(T)	1.292 (1.292)	2,971(2,967)				98.4 (97.3)
	aug-pVTZ	CCSD(T)	1.279 (1.279)	2,991(2,988)				105.0 (103.9)
Ref. [104]	aug-pVTZ	MBPT(4)+R	1.282	3,009				
Ref. [96]	aug'-cc-pV(n+d)Z	W4(CCSDTQ)	1.274	2,991.50				
Ref. [102]		Experiment						102.21
Ref. [101]		Experiment	1.2746	2,989.7				106.4
Ref. [74]		Experiment	1.2746	2,991	53	10.593	0.00053	106.4

See text for details

MRCI+Q: multireference configuration interaction + Davidson correction. CAS-CI: Full-valence complete active space (CAS)-based multireference configuration interaction DK3-CC: Theoretical best estimate obtained from a combination of DK3-CCSD, DK3-CCSDT, DK3-CCSDTQ with the cc-pVDZ, cc-pVTZ, and cc-pVQZ basis sets [68]

Refs. [83, 84]: Values within the parenthesis correspond to the calculations made by the Dirac-Coulomb-(Gaunt) Hamiltonian.  $\Delta$ : Corresponds to the deviation of SS-MRMPPT/aug-cc-pVTZ with respect to the experimental results

approaches are much more expensive than the SS-MRMPPT calculations. As far as the computational cost is concerned, the shape of the SS-MRMPPT surface is competitive with the results of CCSDT and CR-CCSD(T) ones. From the figure, it is clear that there is no unphysical hump along the elongation coordinates of the SS-MRMPPT energy surface of  $X^1\Sigma^+$  HCl system. It is worth mentioning that Piecuch et al. [100] reported that the well-pronounced nonphysical hump has been found in the CCSD(T) [CCSD perturbatively corrected for triples] surface at  $\sim 2.5$  Å. This inability of the CCSD(T) method is primarily due to the breakdown (or at least inadequacy) of the SR perturbation theory in the presence of MR nature. Thus, our SS-MRMPPT removes or at least attenuates the failure of CCSD(T) in MR situations at expense of low computational cost.

The spectral or molecular constants calculated from the SS-MRMPPT surfaces for two basis sets are given in Table 2. For the sake of completeness of comparison we have also tabulated the corresponding experimental values [74, 101, 102] in Table 2 along with other available theoretical estimates. The results of Hirata et al. [68] and of Klopper et al. [92] are very useful to judge the accuracy of our present SS-MRMPPT results. The main features of the results given in Table 2 may be summed up as follows:

1. Inspection of Table 2 shows that the equilibrium bond distance and the dissociation energy calculated by SS-MRMPPT decrease with increase in the size of basis set whereas the vibrational frequency increases. Thus, the calculated results are systematically convergent to experimental data with respect to the size of basis sets.

- The spectral constants such as  $R_e$ ,  $\omega_e$ ,  $\omega_e x_e$ ,  $B_e$ ,  $D_e$ , and  $D_0$  calculated with the SS-MRMPPT(2,2)/aug-cc-pVTZ model reproduce the experimental data [74] within 0.001 Å, 27, 4, 0.10, 0 cm<sup>-1</sup>, and 0.9 kcal/mol, respectively.
- The differences of our SS-MRMPPT(2,2)/aug-cc-pVTZ values with respect to the best estimated results (DK3-CC) due to Hirata et al. [68] are not very significant (such as  $R_e = 0.002$  Å,  $\omega_e = 27$  cm<sup>-1</sup>,  $\omega_e x_e = 6$  cm<sup>-1</sup>,  $B_e = 0.05$  cm<sup>-1</sup>,  $D_e = 0$  cm<sup>-1</sup>, and  $D_0 = 5.6$  kcal/mol).
- From the values of the molecular constants of  $X^1\Sigma^+$  HCl calculated by Visscher et al. [83, 84] using various non-relativistic and relativistic methods, it is clear that the calculated molecular constants show very little change upon inclusion of relativity. It is apparent that our computed  $R_e$  and  $\omega_e$  are in very satisfactory agreement with the CCSD(T) and CISD+Q results of Visscher et al. [83, 84] illustrating the accuracy of the SS-MRMPPT method.
- As is evident from the table, the SS-MRMPPT molecular constants are in line with previous computations of MRCI+Q [99].
- Our results are in good agreement with the MRD-CI (multireference double-excitation configuration interaction) as well as SA-CASSCF-CI with ECP basis sets (effective core potentials with state-averaged CASSCF-CI) and are very close to CEPA (coupled-electron pair approximation) methods [97].
- It is interesting to note that CAS-BCCC4 (block correlated CC method with a CASSCF reference function with truncation up to the four-block correlation level) [98] predictions listed in Table 2 are in close agreement with our computed results.
- Table 2 also shows that our SS-MRMPPT spectroscopic parameters are in qualitative agreement with full-valence complete active space-based multireference configuration interaction (CAS-CI) results [ $R_e = 1.2751$  Å, and  $D_0 = 105.7$  kcal/mol] due to Woon and Dunning [103] at the cost of low computational effort. The dimension of CAS used in their CI calculations is larger than ours CAS(2,2).
- The computed molecular constants via SS-MRMPPT/aug-cc-pVTZ calculations are also in good agreement with the results of Klopper et al. [92] performed at full-blown computationally expensive CCSD(T)(Full)/aug-cc-pV5Z+DPT(CCSD)level. The difference between these two calculations is around  $R_e = 0.002$  Å,  $\omega_e = 24$  cm<sup>-1</sup>,  $\omega_e x_e = 2.6$  cm<sup>-1</sup>, and  $B_e = 0.12$  cm<sup>-1</sup>.

### 2.3 Ground-state hydrogen bromide [ $X^1\Sigma^+$ HBr]

The spectroscopic information about HBr would be helpful for monitoring the ozone layer depletion, as this molecule

plays an important role in the depletion mechanism. In metrology, transition frequencies of this molecule can be used to calibrate the spectrometers and tunable laser devices. Since HBr plays an important role in the depletion mechanism, the information on this molecule would be helpful for monitoring the ozone layer depletion. Hence, it is not a surprise that a number of theoretical [68, 83, 84, 104–107]<sup>17</sup> (for an excellent illustration of the performance by the various approaches for HBr see [108]) and experimental [74, 109, 110] investigations have been carried out for the  $X^1\Sigma^+$  HBr molecule in the past several years. Of these investigations, however, only a few experiments and theories are involved in evaluating the ground-state spectroscopic properties of  $X^1\Sigma^+$  HBr. The spectroscopic properties of the HBr molecule are significantly influenced by relativistic effects and electron correlation. Thus, it is very constructive to demonstrate the capability of the (non-relativistic) SS-MRMPPT method in calculating the complete PES of the  $X^1\Sigma^+$  HBr molecule. For the HBr molecule, we use basis sets of a aug-cc-pVDZ and aug-cc-pVTZ quality. In our post mean-field calculations, we do not correlate the Ne-like core on Br. Over the internuclear distance range considered here, the obtained SS-MRPT energy surface is both smooth and completely convergent indicating the robustness of the method.

Table 3 is a compendium of results for various methods including our present SS-MRMPPT ones. In Table 3, we also include the results of relativistic calculation by other methods to show the influence of relativity. A comparison with the all-electron CCSD(T)/cc-pV5Z-DK results [107]<sup>18</sup> is also shown in Table 3. The relative qualities of our computed results in the case of the HBr molecule may be addressed as follows:

- We observe that the SS-MRMPPT/aug-cc-pVTZ modulates the SS-MRMPPT/aug-cc-pVDZ spectroscopic constants (except dissociation energy) by just the adequate amount toward the experimental data.
- The errors of our computed  $R_e$ ,  $\omega_e$ ,  $\omega_e x_e$ ,  $B_e$ ,  $D_e$  and  $D_0$  with respect to the experimental values are 0.002 Å, 40.03 cm<sup>-1</sup>, 4 cm<sup>-1</sup>, 0.04 cm<sup>-1</sup>, 0.00002 cm<sup>-1</sup> and

<sup>17</sup> The results reported in this paper provide very accurate and complete investigations on the molecular parameters of the  $X^1\Sigma^+$  HBr when compared with the previous theoretical estimations. Their results almost perfectly conform to the available experimental measurements.

<sup>18</sup> In this paper, Peterson et al. performed the  $D_0$ ,  $R_e$ ,  $\omega_e$  and  $\omega_e x_e$  calculations by the CCSD(T) method with a series of correlation-consistent basis sets in conjunction with small-core relativistic pseudopotentials, aug-cc-pVnZ-PP ( $n = 2, 3, 4, 5$ ). In order to assess the impact of the pseudopotential approximation on the calculated properties, they also made the all-electron CCSD(T) Douglas–Kroll–Hess calculations using the correlation-consistent quintuple basis set augmented with diffused functions, aug-cc-pV5Z-DK.



- 6.51 kcal/mol, respectively. The corresponding errors for DK3-CC [68] are 0.001 Å, 14, 2, 0.0, 0.0001 cm<sup>-1</sup> and 4.14 kcal/mol, respectively. The deviations of  $R_e$ ,  $\omega_e$ , and  $D_0$  provided by CCSD(T)/aug-cc-pV5Z-DK scheme [107] from the experiment values are 0.005 Å (overestimated), 2.98 cm<sup>-1</sup> (underestimated), and 1.14 kcal/mol (underestimated), respectively. The deviations of MRCI/aug-cc-pV5Z values [108] from the experimental data are:  $R_e = 0.005$  Å,  $\omega_e = 8.68$  cm<sup>-1</sup>, and  $D_0 = 0.18$  kcal/mol. It should be mentioned that the full-valence CASSCF has been employed by Shi et al. [108] as the reference wavefunction for their MRCI calculations.
3. Visscher et al. [83, 84] have observed that the inclusion of relativistic effect leads to a weakening of the bond by about 0.002 Å, leading to a decrease in the calculated harmonic frequencies by approximately 14 cm<sup>-1</sup> and dissociation energies by about 4 kcal/mol for  $X^1\Sigma^+$  HBr in the case of MP2, CISD, CISD+Q, and CCSD(T) methods. Keeping in mind the differences in relativistic treatments, basis sets, and correlation methods, their results and our SS-MRMPPT results are in acceptably good agreement.
  4. From Table 3, we see that the spectroscopic parameters provided by the SS-MRMPPT results are in relatively good agreement with the computationally expensive CCSD(T), CCSDT, and MRCI results.
  5. The deviations of SS-MRMPPT/aug-cc-pVTZ from the best estimated complete-correlation, complete-basis-set results of Hirata et al. are  $R_e$  (Å) = 0.003,  $\omega_e$  (cm<sup>-1</sup>) = 26,  $\omega_e x_e = 2$  (cm<sup>-1</sup>),  $B_e$  (cm<sup>-1</sup>) = 0.27,  $D_e$  (cm<sup>-1</sup>) = 0.00001 and  $D_0$ (kcal/mol) = 10.65.
  6. Table 3 also shows the results for the HBr molecule obtained by using aug-cc-pVTZ basis set at the SS-MRMPPT level are in promising agreement with the CCSD(T)/(Full)+DPT(CCSD) findings [92] as is evident from their deviations:  $R_e$  (Å) = 0.001,  $\omega_e$  (cm<sup>-1</sup>) = 11,  $\omega_e x_e = 1.7$ ,  $B_e$ (cm<sup>-1</sup>) = 0.09.
  7. Our SS-MRMPPT/aug-cc-pVTZ  $R_e$ ,  $\omega_e$  and  $D_0$  results are in quite a good agreement with the CCSD(T)/aug-cc-pV5Z-DK [107] data of 1.4189, 2646.9, and 92.78, respectively. In the SS-MRMPPT(2,2)/aug-cc-pVTZ model, the equilibrium bond length underestimates the experimental one by 0.002 Å, whereas the frequency and dissociation energy are overestimated over the experimental measurements by  $\approx 40$  cm<sup>-1</sup> and 6.51 kcal/mol, respectively.
  8. The molecular constants calculated by Lee and Lee [111] [using Kramers' restricted MP2(KRMP2)] are  $R_e = 1.411$  Å,  $\omega_e = 2702$  cm<sup>-1</sup>, and  $D_0 = 83.5$  kcal/mol. Their calculated  $R_e$  and  $\omega_e$  are in line with our results. The KRMP2 dissociation energy is significantly lower than our calculated value with respect to the experimental value.
  9. The deviations of the SOF-CCSDT/TZ+ $\Delta_{SO}$  (SOF-CCSDT/TZ with 18 correlated electrons) spectral constants relative to the experiment are  $R_e = 0.0001$  (0.0002) Å,  $\omega_e = 8.43$  (14.93) cm<sup>-1</sup>, and  $D_0 = 3.46$  (2.08) kcal/mol (see [106]). The corresponding deviations provided by our SS-MRMPPT/aug-cc-pVTZ calculations are 0.002 Å, 40.03 cm<sup>-1</sup>, and 6.51 kcal/mol, respectively.

The above analysis (considering an overall performance) convincingly reveals that the computed spectroscopic constants are generally less accurate than for HCl and HF with respect to the corresponding experimental ones. It appears that the aug-cc-pVXZ basis sets for Br behave somewhat different from the aug-cc-pVXZ basis sets for F and Cl. Not only since the aug-cc-pVXZ sets for Br seem to be less accurate than the corresponding for F, but also in series of diatomics HF, HCl, and HBr, relativistic effects become more and more important and adequate descriptions of the systems containing heavy elements such as bromine require a relativistic electronic structure approach, we expect the evaluated spectroscopic constant for HBr to be less close to the experimental values than for HCl and HF.

In order to investigate the impact of the scalar relativistic corrections on the spectroscopic constants of HBr, Yockel and Wilson [112] have performed the CCSD(T) calculations in combination with the DK contracted correlation-consistent basis sets and small-core relativistic pseudopotentials with the correlation-consistent polarized valence basis sets. The  $R_e$  and  $D_0$  values they have obtained for the ground-state HBr at the aug-cc-pV5Z-PP basis set are of 1.419 Å and 85.39 kcal/mol, respectively. Although the harmony of our  $R_e$  value with Yockel and Wilson [112] one is very good, the deviation of  $D_0$  value is noticeable. Overall, the entries assembled in the table indicate that the SS-MRMPPT investigations on the  $X^1\Sigma^+$  HBr are reliable and acceptably accurate. This is caused by the correct shape of the PES provided by SS-MRMPPT calculations. The SS-MRMPPT equilibrium bond length as well as dissociation energy increase, whereas the frequency decreases with an increase in the size of the basis set. We also found that an elongation of the bond is accompanied by a reduction of the harmonic frequency due to the increase of basis size. Klopper et al. [92] have stated that although the relativistic effects are larger for HBr than HF and HCl, the incompleteness errors inherent in the correlation treatment and truncation of one-particle basis set are seen to dominate the overall deviation of molecular parameters from the experimental ones.

**Table 3** Spectroscopic constants [equilibrium bond length  $R_e(\text{\AA})$ , vibrational frequency  $\omega_e(\text{cm}^{-1})$ , anharmonicity constant  $\omega_e x_e(\text{cm}^{-1})$ , rotational constant  $B_e(\text{cm}^{-1})$ , centrifugal distortion constants  $D_e(\text{cm}^{-1})$ , and dissociation constant  $D_0(\text{kcal/mol})$ ] for the ground state of  $X^1\Sigma^+$  HBr system

Ref.	Basis	Methods	$R_e$	$\omega_e$	$\omega_e x_e$	$B_e$	$D_e$	$D_0$
This work	aug-cc-pVDZ	SS-MRMPPT(2,2)	1.402	2,724	49	8.55	0.00033	94.1
	aug-cc-pVTZ	SS-MRMPPT(2,2)	1.412	2,689	49	8.43	0.00033	96.9
$\Delta$			0.002	40.03	4	0.04	0.00002	6.51
Ref. [106]	TZ	SO MRCISD (8)	1.4187	2,634.9				86.94
	TZ	SO MRCCSD (8)	1.4193	2,630.6				86.70
	TZ	SOF CCSDT (18)	1.4142	2,663.9				92.47
	TZ	SOF CCSDT (18)+ $\Delta_{\text{SO}}$	1.4143	2,657.4				86.93
Ref. [108]	aug-cc-pV5Z	MRCI	1.4195	2,642.68				90.57
Ref. [107]	aug-cc-pVDZ-PP	CCSD(T)	1.4290	2,641.4	46.7			88.17
	aug-cc-pV5Z-PP	CCSD(T)	1.4190	2,646.3	44.9			92.78
	aug-cc-pV5Z-DK (all-electron)	CCSD(T)	1.4189	2,646.9	45.0			92.78
Refs. [83, 84]	aug-pVDZ	CISD+Q	1.429 (1.427)	2,655 (2,641)				88.6 (84.8)
	aug-pVTZ	CISD+Q	1.421 (1.419)	2,662 (2,646)				91.1 (87.2)
	aug-pVDZ	CCSD(T)	1.429 (1.427)	2,659 (2,646)				89.0 (85.2)
	aug-pVTZ	CCSD(T)	1.421 (1.419)	2,660 (2,645)				92.0 (88.1)
Ref. [104]	aug-pVTZ	MBPT(4)+R	1.421	2,693				
Ref. [105]	Basis1	Relativistic CI	1.455	2,645				85.8
Ref. [68]	cc-pVTZ	DK3-CCSD	1.418	2,657	46	8.422	0.00034	88.09
	cc-pVDZ	DK3-CCSDT	1.432	2,632	48	8.253	0.00032	83.78
	cc-pVTZ	DK3-CCSDT	1.421	2,634	47	8.392	0.00034	89.32
	cc-pVDZ	DK3-CCSDTQ	1.433	2,631	48	8.251	0.00032	80.02
		DK3-CC	1.415	2,663	47	8.457	0.00034	86.25
Ref. [92]	aug-cc-pCVQZ	CCSD(T)+DPT(CCSD)	1.4104	2,677.9	47.3	8.52		
Ref. [112]	aug-cc-pV5Z-PP	CCSD(T)	1.419				85.39	
Ref. [74]		Experiment	1.4144	2,648.97	45 (5)	8.465	0.00035	90.39

See text for details

DK Douglas–Kroll–Hess

Basis1: A triple-zeta Slater-type basis set with two polarization functions. DZ and TZ of Ref. [106]: The smaller set DZ consists of the sp-pvdz set from the MOLFDIR suite in the DIRAC program package for Br (15s12p6d) and H (4s1p). The larger set TZ is the relativistic finite nucleus optimized triple-zeta basis set including valence-correlating functions for Br (23s16p10d1f) and the cc-pVTZ of the MOLCAS package for H (5s2p1d).  $\Delta_{\text{SO}}$  spin-orbit shift

Refs. [83, 84]: Values within the parenthesis correspond to the calculations made by the Dirac-Coulomb-(Gaunt) Hamiltonian. DK3-CC: Theoretical best estimate obtained from a combination of DK3-CCSD, DK3-CCSDT, DK3-CCSDTQ with DZ, TZ, and QZ [68]

$\Delta$ : Corresponds to the deviation of SS-MRMPPT/aug-cc-pVTZ with respect to the experimental results

### 3 General discussion

The calculated values of the dissociation energy via SS-MRMPPT computations exhibit the trend  $\text{HF} > \text{HCl} > \text{HBr1}$ , as is also observed experimentally, as it should be. From our present computations, it is quite evident that the estimated equilibrium bond distances via SS-MRMPPT agree well with the experimental trend for the HX systems, that is,  $R_{\text{H-Br}} > R_{\text{H-Cl}} > R_{\text{H-F}}$ .

The results (*vide supra*) unequivocally suggest that the SS-MRMPPT approach can provide a quite well-balanced description of energetics of electronic states along bond breaking coordinates for this class of chemical species as the differences between the results of the SS-MRMPPT and latest generation high-level methods are acceptably small for all species studied. This can be traced back to the fact that the wave function of a diatomic hydride with its bond significantly stretched assumes a two-determinant

character, and SS-MRMPPT is capable of describing the electron correlation in an accurate manner over the entire dissociation energy surface. It is worth noting that the description of bond stretched hydrides affects the shape of PES to the extent that the calculated spectroscopic constants at the equilibrium bond lengths have appreciable errors [68]. While SS-MRPT method naturally fixes the failures of standard single-reference methods and is being recently applied with a good degree of success to study electronic states and energy surfaces of molecules displaying pronounced multireference character, it inevitably also has some limitations and difficulties which need to be addressed. There is also a potential source of numerical instability in the working equations of SS-MRPT theory. Considering Eq. (2), we see that division by the reference expansion coefficient  $c_\mu$  in the numerator in certain circumstances may give rise to numerical instability when  $c_\mu$  is much smaller compared to  $c_\nu$  (lead to rather large values for  $T_\mu$ , which in turn introduces instability to  $\tilde{H}_{\mu\nu}^{(2)}$ ) [46, 113–116]. The situation becomes more severe with increasing size of the CAS, since many  $c_\mu$ 's are close to zero at one point of the potential energy curve or another. A similar fact has also been reported in the parent SS-MRCC theory [28] as well as in a related MRCC theories developed by Hanrath [117] while SUMR- and BWMR-based methods do not contain the  $c_\mu$  weight in the denominator. To get rid of this problem, various schemes have been suggested and implemented [113, 114].<sup>19</sup> Thanks to the fact that the variety of systems and CAS that we have used till now (including the present work) to implement the SS-MRMPPT method have illustrated that the method does not face severe numerical instability of the amplitude determining equations even when all the coefficients are being included. Another obvious bottleneck of CAS-based method is that the computational cost rises exponentially with the size of active space, limiting

<sup>19</sup> Also, it has not escaped our attention that to eliminate or considerably reduce the numerical instability of the cluster amplitudes equations of the SS-MRMPPT approach, one can use Tikhonov regularization scheme [115], where replaces  $\frac{1}{c_\mu}$  in the coupling term of Eq. (2) by  $\frac{1}{\tilde{c}_\mu}$ :

$$\frac{1}{\tilde{c}_\mu} = \frac{c_\mu}{c_\mu^2 + \tau^2}$$

where  $\tau$  is a parameter set by users and is a real quantity. It is evident that  $\frac{1}{\tilde{c}_\mu} = \frac{1}{c_\mu}$  when  $c_\mu$  has a large value while  $\frac{1}{\tilde{c}_\mu} = \frac{c_\mu}{\tau^2}$  for very small value of  $c_\mu$ . However, at present we have not incorporated this scheme in our code. We are now engaged in such an implementation which we intend to present in near future. It is worth mentioning at this juncture that the special care for the treatments of the amplitude equation in conjunction with very small value of the reference coefficients are not necessary for the unrelaxed description of the SS-MRMPPT method (see [47, 48]).

practical calculations to small active spaces (as that of other CAS-based methods). The internally contracted CAS approach [118–122] (that can ameliorate the computational costs since its scale much lower than uncontracted methods) has evolved as a potential alternative that holds the promise to bypass or at least to attenuate this shortcoming. Among the perturbative methods the CIPSI code [16–18] is internally contracted and externally decontracted and so are its numerous variants. The popular and efficient CASPT2 method [6–8] is both internally and externally contracted, and so is the NEVPT second-order expansion [19–22]. Moreover, similar to most MRPT's, SS-MRPT does not conserve orbital invariance of the underlying CAS wavefunction neither in its original form [28, 29], nor in a reformulation suggested by various workers [39–45]. We should point out at this stage that the JM ansatz applied to a CAS reference function does not show orbital invariance with respect to the transformation among the active orbitals. As already numerically alluded by Mahapatra et al. [39–44] SS-MRMPPT is not invariant to orbital rotations that may leave the reference function unaffected. Recent analysis of the orbital invariance problem due to Evangelista and Gauss [123] has led us to the conclusion that there are intrinsic limitations in the JM ansatz.

#### 4 Concluding remark

The computation of energies and molecular properties for multireference systems with chemical accuracy is one of the most intriguing problems in electronic structure theory and a convincing solution, warranting a balanced treatment of dynamic and static electron correlation, has not been presented yet. Several variants of perturbation theory for MR situations have been proposed, but never turned into a general tool. The state-specific multireference Møller–Plesset perturbation theory, SS-MRMPPT (a Hilbert space method that retains all of the flexibility of the wave function for optimizing the description of a single, target electronic state) tailored particularly for multireference systems possesses several attractive features [size-extensivity, size-consistency (with localized active orbitals), and the potential to be intruder free at the same time] that make it a useful candidate for efficient theoretical descriptions of dissociative phenomena and of many electronically excited states, as well as of ground states in MR systems. It is a multipartitioning generalization of the Møller–Plesset second-order method (MP2) to the cases where the reference function is of the complete active space. It is built on a wave operator formalism, in which the energy is obtained as a root of an effective Hamiltonian. The present computations further emphasize the utility of the method for theoretical descriptions of dissociative phenomena of

ground states in MR systems. Our present applications of SS-MRMPPT method to the single-bond dissociations of HX ( $X = \text{F, Cl, and Br}$ ) molecular systems in their ground state again prove that the method is credible and can be used to perform complete energy surface calculations. Comparing with the estimations of recent generation calculations along with experimental data (whenever available), we found that the present SS-MRMPPT calculations provide acceptably good theoretical investigations on the molecular constants including dissociation energy even with the physically motivated smallest possible CAS [i.e., CAS(2,2)] and at an expense of low computational cost that make it a serious candidate for efficient handling of electron correlation in MR-based methods. The pattern of variation of spectroscopic constants with the size of the basis sets is very encouraging. Our present studies in the case of HF molecule clearly indicate that the SS-MRMPPT results systematically improve when extending the basis set and, in the CBS limit, best approximate the experimental results. The work presented here shows that correlation-consistent basis sets provide a systematic series of basis sets of increasing accuracy and completeness. We should also mention here that our previously published results [39–44] along with the present one have showed that the relative accuracy of the computed energy via SS-MRPT in a wide range of distances on the PESs was also non-uniform, which is obviously not desirable. However, the non-uniformity is not significant in general. This is also the case for other MRPT calculations in conjunction with small CAS. In fact, the overall accuracy of the present calculations is limited by the perturbatively approximated non-relativistic wavefunction model. Even though more calculations with complete-correlation complete-basis-set extrapolated potential surfaces along with the analysis of the spectroscopic constants derived from these surfaces are certainly needed to fully assess the applicability of the approach in calculating PESs and such tests will be performed in the near future, the results presented in this work indicate that the approach has the capability of delivering promising accuracy. In near future, we will also explore more examples to show how SS-MRMPPT (and its internal contracted variant) calculations can have an impact on interesting and computationally challenging molecular systems. It is worth stressing that unfavorable computational scaling with the size of the active space is another formal deficiency of CAS-based methodologies which limits their applicability to small active spaces. A solution to the problem that afflict methods based on the CAS requires the consideration of an alternative wave function parameterization. A straightforward solution is to adopt a contracted description of the ansatz of the starting wave function as that of the contracted MRCI method. Such a scheme in the context of SS-MRPT approach has already

been accomplished in our group and the results will be published very soon.

**Acknowledgments** This paper is dedicated to Professor Shankar Prasad Bhattacharyya, a great teacher, at the occasion of his reaching sixty-five. We have all benefited immensely from our interactions over the years with him. We thank Dr. Debi Banerjee for critical reading of the manuscript. This work has been funded by the Department of Science and Technology of India [Grant No. SR/S1/PC-61/2009]. S.C. acknowledges the infrastructural facility developed in his department through UGC-SAP program.

## References

1. Dykstra CE, Frenking G, Kim KS, Scuseria GE (eds) (2005) In: Theory and Applications of Computational Chemistry: The First 40 Years. Elsevier, Amsterdam
2. Shavitt I (1998) 94:3 and references therein
3. Shavitt I, Bartlett RJ (2009) In: Many-Body Methods in Chemistry and Physics: MBPT and Coupled-Cluster Theory, Cambridge University Press, Cambridge
4. Møller M, Plesset MS (1934) Phys Rev 46:618
5. Pople JA, Binkley JS, Seeger R (1976) Int J Quantum Chem S 10:1
6. Andersson K, Malmqvist PÅ, Roos BO, Sadlej AJ, Wolinski K (1990) J Chem Phys 94:5483
7. Andersson K, Malmqvist PÅ, Roos BO (1992) J Chem Phys 96:1218
8. Gagliardina L, Roos B (2007) Chem Soc Rev 36:893 and references therein
9. Hirao K (1992) Chem Phys Lett 190:374
10. Hirao K (1992) Chem Phys Lett 196:397
11. Nakao Y, Choe YK, Nakayama K, Hirao K (2002) Mol Phys 100:729
12. Choe Y-K, Nakao Y, Hirao K (2001) J Chem Phys 115:621
13. Nakano H (1993) J Chem Phys 99:7983
14. Hoffmann MR (1992) Chem Phys Lett 195:127
15. Jiang W, Khait YG, Hoffmann MR (2009) J Phys Chem A 113:4374
16. Huron B, Malrieu JP, Rancurel P (1973) J Chem Phys 58:5745
17. Evangelisti S, Daudey JP, Malrieu JP (1983) Chem Phys 75:91
18. Angeli C, Cimraglia R, Persico M, Toniolo A (1997) Theor Chem Acc 98:57
19. Angeli C, Cimraglia R, Evangelisti S, Leininger T, Malrieu JP (2001) J Chem Phys 114:10252
20. Angeli C, Borini S, Cimraglia R (2004) Theor Chem Acc 111:352
21. Angeli C, Pastore M, Cimraglia R (2007) Theor Chem Acc 117:743
22. Pastore M, Angeli C, Cimraglia R (2007) Theor Chem Acc 118:35
23. Hubač I, Mach P, Wilson S (2002) Mol Phys 100:859
24. Papp P, Mach P, Hubač I, Wilson S (2007) Int J Quantum Chem 107:2622
25. Papp P, Neogrady P, Mach P, Pittner J, Hubač I, Wilson S (2008) Mol Phys 57:106
26. Rolik Z, Szabados Á, Surján P R (2003) J Chem Phys 119:1922
27. Szabados Á, Rolik Z, Tóth G, Surján PR (2005) J Chem Phys 122:114104
28. Mahapatra US, Datta B, Mukherjee D (1999) J Chem Phys 110:6171
29. Mahapatra US, Datta B, Mukherjee D (1999) J Phys Chem 103:1822



30. Chen F, Davidson ER, Iwata S (2002) *Int J Quantum Chem* 86:256
31. Angeli C, Cimiraglia R, Malrieu J-P (2006) *Theor Chem Acc* 116:434
32. Chaudhuri RK, Freed KF, Chattopadhyay S, Mahapatra US (2008) *J Chem Phys* 128:144304
33. Chattopadhyay S, Chaudhuri RK, Mahapatra US (2008) *J Chem Phys* 129:244108
34. Chattopadhyay S, Chaudhuri RK, Freed KF (2011) *Phys Chem Chem Phys* 13:7514
35. Shahi ARM, Cramer CJ, Gagliardi L (2009) *Phys Chem Chem Phys* 11:10964
36. Granovsky AA (2011) *J Chem Phys* 134:214113
37. Roskop L, Gordon MS (2011) *J Chem Phys* 135:044101
38. Pahari D, Chattopadhyay S, Das S, Mukherjee D, Mahapatra US (2005). In: Dykstra CE, Frenking G, Kim KS, Scuseria GE (eds) *Theory and applications of computational chemistry: the first 40 years*, Elsevier, Amsterdam, p 581
39. Mahapatra US, Chattopadhyay S, Chaudhuri RK (2008) *J Chem Phys* 129:024108
40. Mahapatra US, Chattopadhyay S, Chaudhuri RK (2009) *J Chem Phys* 130:014101
41. Chattopadhyay S, Mahapatra US, Chaudhuri RK (2009) *J Phys Chem A* 113:5972
42. Mahapatra US, Chattopadhyay S, Chaudhuri RK (2010) *J Chem Theory Comput* 6:662
43. Chattopadhyay S, Mahapatra US, Chaudhuri RK (2010) *Chem Phys Lett* 488:229
44. Mahapatra US, Chattopadhyay S, Chaudhuri RK (2010) *J Phys Chem A* 114:3668
45. Evangelista FA, Simmonett AC, Schaefer HF III, Mukherjee D, Allen WD (2009) *Phys Chem Chem Phys* 11:4728
46. Hoffmann MR, Datta D, Das S, Mukherjee D, Szabados Á, Rolik Z, Surján PR (2009) *J Chem Phys* 131:204104
47. Mao S, Cheng L, Liu W, Mukherjee D (2012) *J Chem Phys* 136:024106
48. Mao S, Cheng L, Liu W, Mukherjee D (2012) *J Chem Phys* 136:024105
49. Schucan TH, Weidenmüller HA (1973) *Ann Phys (NY)* 76:483
50. Finley JP, Freed KF (1995) *J Chem Phys* 102:1306
51. Kowalski K, Piecuch P (2000) *Phys Rev A* 61:052506
52. Van Dam HJJ, Van Lenthe JH, Ruttnik PJA (1999) *Int J Quantum Chem* 72:549
53. Witek HA, Nakano H, Hirao K (2003) *J Chem Phys* 118:8197
54. Rintelman JM, Adamovic I, Varganov S, Gordon MS (2005) *J Chem Phys* 122:044105
55. Azizi Z, Roos BO, Veryazova V (2006) *Phys Chem Chem Phys* 8:2727
56. Chaudhuri RK, Freed KF, Hose G, Piecuch P, Kowalski K, Wloch M, Chattopadhyay S, Mukherjee D, Rolik Z, Szabados A, Toth G, Surjan PR (2005) *J Chem Phys* 122:134105
57. Zaitsevskii A, Malrieu JP (1995) *Chem Phys Lett* 233:597
58. Rolik Z, Szabados Á (2009) *Int J Quantum Chem* 109:2554
59. Zaitsevskii A, Malrieu JP (1997) *Theor Chem Acc* 96:269
60. Jeziorski B, Monkhorst HJ (1981) *Phys Rev A* 24:1668
61. Jeziorski B (2010) *Mol Phys* 108:3043
62. Finley J, Malmqvist P-Å, Roos BO, Serrano-Andrés L (1998) *Chem Phys Lett* 288:299
63. Shiozaki T, Györfly W, Celani P, Werner H-J (2011) *J Chem Phys* 135:081106
64. Camacho C, Cimiraglia R, Witek HA (2010) *Phys Chem Chem Phys* 12:5058
65. Camacho C, Witek HA, Cimiraglia R (2010) *J Chem Phys* 132:244306
66. Olsen J, Fülischer M P (2000) *Chem Phys Lett* 326:225
67. van Dam HJJ, van Lenthe JH (1997) *Mol Phys* 90:1007
68. Hirata S, Yanai T, de Jong WA, Nakajima T, Hirao K (2004) *J Chem Phys* 120:3297
69. Dunning TH Jr (1989) *J Chem Phys* 90:1007
70. Woon DE, Dunning TH Jr (1993) *J Chem Phys* 98:1358
71. Wilson AK, Woon DE, Peterson KA, Dunning TH Jr (1999) *J Chem Phys* 110:7667
72. Feller D (1996) *J Comput Chem* 17:1571
73. Schuchardt KL, Didier BT, Elsethagen T, Sun L, Gurumoorthi V, Chase J, Li J, Windus TL (2007) *J Chem Inf Model* 47:1045
74. Huber KP, Herzberg G (1979) In: *Constants of Diatomic Molecules*. Van Nostrand Reinhold, New York
75. Schmidt MW, Baldrige KK, Boatz JA, Elbert ST, Gordon MS, Jensen JH, Koseki S, Matsunaga N, Nguyen KA, Su S, Windus TL, Dupuis M, Montgomery JA (1993) *J Comput Chem* 14:1347
76. Gordon MS, Schmidt MW (2005). In: Dykstra CE, Kim KS, Frenking G, Scuseria GE (eds) *Theory and applications of computational chemistry: the first 40 years of quantum chemistry*, Elsevier, Amsterdam, pp 1167–1189
77. Dunham JL (1932) *Phys Rev* 41:721
78. Martin JML (1998) *Chem Phys Lett* 292:411
79. Müller H, Franke R, Vogtner S, Jaquet R, Kutzelnigg W (1998) *Theor Chem Acc* 100:85
80. Li X, Paldus J (1998) *J Chem Phys* 108:637
81. Li X, Paldus J (2000) *Int J Quantum Chem* 80:743
82. Li X, Paldus J (2006) *J Chem Phys* 124:174101
83. Visscher L, Styszyński J, Nieuwpoort WC (1996) *J Chem Phys* 105:1987
84. Styszyński (2000) *J Chem Phys Lett* 317:351
85. Chaudhuri RK, Freed KF, Abrash SA, Potts DM (2001) *J Mol Struct (Theochem)* 547:83
86. Dutta A, Sherrill CD (2003) *J Chem Phys* 118:1610
87. Kowalski K, Piecuch P (2004) *J Chem Phys* 120:1715
88. Paap P, Mach P, Pittner J, Wilson S, Hubač I, Wilson S (2006) *Mol Phys* 104:2367
89. Engels-Putzka A, Hanrath M (2009) *J Mol Struct (Theochem)* 902:59
90. Hirata S, Bartlett RJ (2000) *Chem Phys Lett* 321:216
91. Shiozaki T, Valeev EF, Hirata S (2009) *J Chem Phys* 131:044118
92. Hennen AC, Halkier A, Klopper W (2001) *J Mol Struct* 599:153
93. Kobayashi M, Szabados Á, Nakai H, Surján PR (2010) *J Chem Theory Comput* 6(7):2024
94. Klimentko TA, Ivanov VV, Lyakh DI, Adamowicz L (2010) *Chem Phys Lett* 493:173
95. Das S, Kállay M, Mukherjee D (2011) *Chem Phys* 392:83
96. Karton A, Martin JML (2010) *J Phys Chem* 133:144102
97. Adams GF, Chabalowski CF (1994) *J Phys Chem* 98:5878
98. Shen J, Fang T, Hua W, Li S (2008) *J Phys Chem A* 112:4703
99. Deskevich MP, Hayes MY, Takahashi K, Skodje RT, Nesbitt DJ (2006) *J Chem Phys* 124:224303
100. Piecuch P, Hirata S, Kowalski K, Fan P-D, Windus TL (2006) *Int J Quantum Chem* 106:79
101. Herzberg G (1950) In: *Molecular spectra and molecular structure. I. Diatomic molecules*, 2nd edn. Van Nostrand Reinhold, New York
102. Michel M, Korolkov MV, Weitzel K-M (2002) *Phys Chem Chem Phys* 4:4083
103. Woon DE, Dunning TH (1993) *J Chem Phys* 99:1914
104. Kellö V, Sadlej AJ (1990) *J Chem Phys* 93:8122
105. Chapman DA, Balasubramanian K, Lin SH (1987) *Chem Phys* 118:333
106. Fleig T, Sørensen LK, Olsen J (2007) *Theor Chem Acc* 118:347
107. Peterson KA, Figgen D, Goll E, Stoll H, Dolg M (2003) *J Chem Phys* 119:11113

108. Shi D, Sun J, Chen Z, Liu Y, Zhu Z (2009) *J Mol Struct (Theochem)* 913:85
109. Odashima H (2006) *J Mol Spectrosc* 240:69
110. Yench A, Cormack AJ, Donovan RJ, Lawley KP, Hopkirk A, King GC (1998) *Chem Phys* 238:133
111. Lee SY, Lee YS (1991) *Chem Phys Lett* 187:302
112. Yockel S, Wilson AK (2005) *J Chem Phys* 122:174310
113. Hanrath M (2005) *J Chem Phys* 123:84102
114. Engels-Putzka A, Hanrath M (2009) *Mol. Phys.* 107:143
115. Das S, Mukherjee D, Kállay M (2010) *J Chem Phys* 132:074103
116. Szabados A (2011) *J Chem Phys* 134:174113
117. Hanrath M (2005) *J Chem Phys* 123:084102
118. Werner H-J, Knowles PJ (1988) *J Chem Phys* 89:5803
119. Werner H-J (1996) *Mol Phys* 89:645
120. Roos BO (1987) *Adv Chem Phys* 69:399
121. Celani P, Werner H-J (2000) *J Chem Phys* 112:5546
122. Yanai T, Chan GK-L (2006) *J Chem Phys* 124:194106
123. Evangelista FA, Gauss J (2010) *J Chem Phys* 133:044101